Published in Journal of the American Chemical Society (JACS) 127, issue 26, pp. 9612–9624, 2005,
which should be used for any reference to this work

Spectroscopic Characterization of Site-Specific [Fe_4S_4] Cluster Chemistry in Ferredoxin:Thioredoxin Reductase: Implications for the Catalytic Mechanism

Elizabeth M. Walters,[†] Ricardo Garcia-Serres,[‡] Guy N. L. Jameson,[‡] Dominique A. Glauser,[§] Florence Bourquin,[§] Wanda Manieri,[§] Peter Schürmann,[§] Michael K. Johnson,*[,†] and Boi Hanh Huynh*[,‡]

Department of Chemistry and Center for Metalloenzyme Studies, University of Georgia, Athens, Georgia 30602
Department of Physics, Emory University, Atlanta, Georgia 30322
Laboratoire de Biochimie Végétale, Université de Neuchâtel, CH-2007 Neuchâtel, Switzerland

Abstract: Light regulation of enzyme activities in oxygenic photosynthesis is mediated by ferredoxin: thioredoxin reductase (FTR), a novel class of disulfide reductase with an active site comprising a $[Fe_4S_4]^{2+}$ cluster and an adjacent disulfide, that catalyzes reduction of the thioredoxin disulfide in two sequential one-electron steps using a $[Fe_2S_2]^{2+/+}$ ferredoxin as the electron donor. In this work, we report on spectroscopic (EPR, VTMCD, resonance Raman, and Mössbauer) and redox characterization of the active site of FTR in various forms of the enzyme, including wild-type FTR, point-mutation variants at each of the active-site cysteine residues, and stable analogues of the one-electron-reduced FTR-Trx heterodisulfide intermediate. The results reveal novel site-specific Fe_4S_4-cluster chemistry in oxidized, one-electron-reduced, and two-electron-reduced forms of FTR. In the resting enzyme, a weak interaction between the Fe_4S_4 cluster and the active-site disulfide promotes charge buildup at a unique Fe site and primes the active site to accept an electron from ferredoxin to break the disulfide bond. In one-electron-reduced analogues, cleavage of the active-site disulfide is accompanied by coordination of one of the cysteine residues that form the active-site disulfide to yield a $[Fe_4S_4]^{3+}$ cluster with two cysteinate ligands at a unique Fe site. The most intriguing result is that two-electron-reduced FTR in which the disulfide is reduced to a dithiol contains an unprecedented electron-rich $[Fe_4S_4]^{2+}$ cluster comprising both valence-delocalized and valence-localized $Fe^{2+}Fe^{3+}$ pairs. These results provide molecular level insights into the catalytic mechanism of FTR, and two viable mechanisms are proposed.

Introduction

Ferredoxin:thioredoxin reductase (FTR) is a novel type of disulfide reductase that plays a central role in light regulation of oxygenic photosynthesis in chloroplasts.[1] FTR functions as a signal transducer, catalyzing the conversion of the light-induced electronic signal in the form of reduced $[Fe_2S_2]$ ferredoxin (Fd) to a chemical signal in the form of the reduced dithiol form of thioredoxins (Trx) *m* and *f*:[2]

$$2Fd_{red} + Trx_{ox} + 2H^+ \rightarrow 2Fd_{ox} + Trx_{red}$$

The reduced Trxs subsequently activate or inactivate a range of target enzymes via dithiol/disulfide exchange to optimize light-dependent metabolism.[1,3] The majority of disulfide reductases in biology are flavoenzymes that function by concerted two-electron steps, using NAD(P)H as the electron donor to reduce an active-site flavin which in turn reduces an adjacent disulfide.[4−6] In contrast, FTR is unique in using a one-electron donor in the form of reduced $[Fe_2S_2]$ Fd and an active site comprising a $[Fe_4S_4]$ cluster in close proximity to an active-site disulfide.[7−9] Understanding the molecular role of the active-site Fe−S cluster in mediating disulfide reduction in two sequential one-electron steps and facilitating substrate reduction promises to reveal new site-specific functionality for biological $[Fe_4S_4]$ clusters.

[†] University of Georgia.
[‡] Emory University.
[§] Université de Neuchâtel.

(1) Buchanan, B. B.; Schürmann, P.; Wolosiuk, R. A.; Jacquot, J.-P. *Photosynth. Res.* **2002**, *73*, 215−222.
(2) Schürmann, P. *Antioxid. Redox Signaling* **2003**, *5*, 69−78.
(3) Balmer, Y.; Koller, A.; del Val, G.; Manieri, W.; Schürmann, P.; Buchanan, B. B. *Proc. Natl. Acad. Sci. U.S.A.* **2003**, *100*, 370−375.
(4) Williams, C. H., Jr. In Chemistry and Biochemistry of Flavoenzymes, Vol. III;M¨uller, F., Ed.; CRC Press: Boca Raton, FL, 1992; pp 121-211.
(5) Williams, C. H., Jr. *FASEB J.* **1995**, *9*, 1267−1276.
(6) Williams, C. H., Jr.; Arscott, L. D.; Müller, S.; Lennon, B. W.; Ludwig, M. L.; Wang, P.-F.; Veine, D. M.; Becker, K.; Schirmer, R. H. *Eur. J. Biochem.* **2000**, *267*, 6110−6117.
(7) Chow, L.-P.; Iwadate, H.; Yano, K.; Kamo, M.; Tsugita, A.; Gardet-Salvi, L.; Stritt-Etter, A.-L.; Schürmann, P. *Eur. J. Biochem.* **1995**, *231*, 149−156.
(8) Staples, C. R.; Ameyibor, E.; Fu, W.; Gaudet-Salvi, L.; Stritt-Etter, A.-L.; Schürmann, P.; Knaff, D. B.; Johnson, M. K. *Biochemistry* **1996**, *35*, 11425−11434.
(9) Dai, S.; Schwendtmayer, C.; Schürmann, P.; Ramaswamy, S.; Eklund, H. *Science* **2000**, *287*, 655−658.

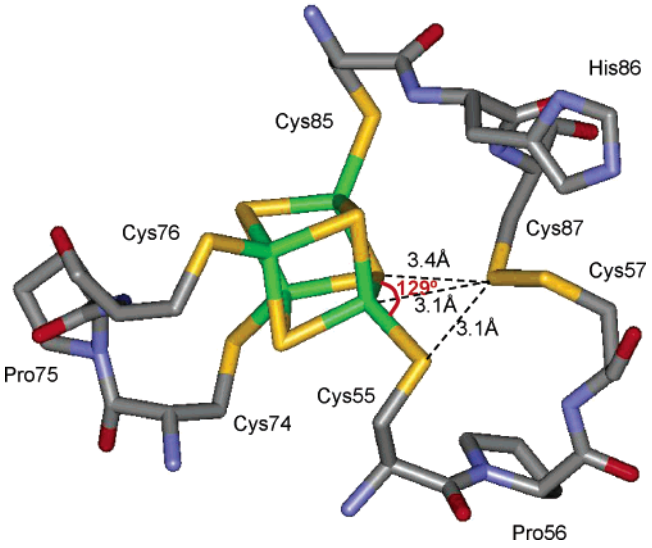

Figure 1. Crystallographically defined active-site structure of *Synechocystis* FTR.[9] Color code: Fe = green; S = yellow; C = gray; N = blue; O = red.

FTR is a heterodimer comprising a highly conserved 13-kDa catalytic subunit, which houses the $[Fe_4S_4]$ cluster and the adjacent disulfide, and a variable subunit of similar or smaller size, which shows little sequence conservation between species.[7,8] *Synechocystis* sp. PCC6803 FTR has been structurally characterized in the oxidized state by X-ray crystallography at 1.6 Å resolution and was found to be a concave disk, 40−50 Å in diameter and 10 Å across at the center.[9] The cluster and disulfide are positioned near the center of the disk with putative binding sites for the $[Fe_2S_2]$ Fd on the $[Fe_4S_4]$ cluster side and for Trx on the disulfide side.[9] Crystallography confirmed the active-site structure deduced from spectroscopic and chemical modification studies of spinach FTR,[7,8,10] comprising a $[Fe_4S_4]$ cluster ligated by four cysteinyl ligands (Cys55, Cys74, Cys76, and Cys85 for *Synechocystis*) adjacent to an asymmetrically disposed disulfide (Cys57 and Cys87 for *Synechocystis*). As shown in Figure 1, the active-site disulfide is very close to the cluster with the S atom of Cys87 3.1 Å from both a cluster Fe and the S atom of the coordinating Cys residue (Cys55) and 3.4 Å from a μ_3-S^{2-}.[9] Moreover, the possibility of a weak interaction between the disulfide and the unique Fe site is suggested by the μ_3-S−Fe−S(Cys55) angle that is opened to 129° and by Mössbauer studies.[11,12]

Spectroscopic studies of wild-type spinach FTR and a chemically modified inactive form, termed NEM-FTR, in which Cys54 (corresponding to Cys57 in *Synechocystis* FTR) is selectively alkylated with *N*-ethylmaleimide (NEM), have provided insight into the catalytic mechanism and the nature of the one-electron-reduced intermediate.[8,10,11] While both the oxidized (disulfide) and the two-electron-reduced (dithiol) forms of FTR contain $S = 0$ $[Fe_4S_4]^{2+}$ clusters, a transient $S = {}^1/_2$ species corresponding to a one-electron-reduced intermediate was observed via freeze-quench EPR studies on reduction with stoichiometric reduced methyl viologen and during catalytic turnover in the presence of Trx, and found to have EPR properties identical to those of oxidized NEM-FTR.[10] Hence, NEM-FTR provides a stable analogue of the one-electron-reduced intermediate, thereby facilitating detailed spectroscopic characterization. The combination of UV−visible absorption, EPR, ^{57}Fe and ^{1}H electron nuclear double resonance (ENDOR), variable-temperature magnetic circular dichroism (VTMCD), resonance Raman, and Mössbauer spectroscopies have shown that NEM-FTR contains a novel type of $S = {}^1/_2$ $[Fe_4S_4]^{3+}$ cluster with an anomalously low redox potential for the $[Fe_4S_4]^{3+/2+}$ couple ($E_m = -210$ mV at pH 7).[8,10,11] The structural and redox properties, coupled with the Mössbauer characterization of oxidized wild-type spinach FTR and oxidized spinach NEM-FTR, which indicate that one-electron reduction is accompanied by site-specific oxidation at a unique Fe site of the $[Fe_4S_4]$ cluster,[11] have led to the proposal that oxidized NEM-FTR and, by analogy, the one-electron-reduced intermediate comprise a $[Fe_4S_4]^{3+}$ cluster with two cysteinate ligands at the unique Fe site (Cys55 and Cys87 in *Synechocystis* FTR; Cys52 and Cys84 in spinach FTR).[11,12] Hence, one-electron reduction can be formally viewed as two-electron reduction of the disulfide with concurrent one-electron oxidation of the cluster due to coordination of an additional cysteinate ligand. This provides a means of anchoring one of the active-site thiol ligands via cluster coordination (the cluster-interacting or electron-transfer thiol), while freeing the other thiol (interchange thiol) for nucleophilic attack of the Trx disulfide to form an FTR/Trx heterodisulfide intermediate. Further one-electron reduction reduces the cluster to the $[Fe_4S_4]^{2+}$ state and releases the electron-transfer thiol to reform the active-site disulfide, with concomitant cleavage of the heterodisulfide and formation of the reduced dithiol form of Trx. The proposed mechanistic scheme is depicted in Figure 2.[12]

The mechanistic scheme shown in Figure 2 predicts specific and noninterchangeable roles for each of the two active-site cysteines and the existence of an FTR/Trx heterodisulfide intermediate analogous to oxidized NEM-FTR. The primary objective of this study was therefore to test these predictions by characterizing the spectroscopic and redox properties of the $[Fe_4S_4]$ clusters in variants involving site-specific mutations of each of the active-site cysteine residues and in a stable heterodisulfide complex involving FTR and an active-site cysteine variant of Trx.[13] To this end, we report EPR, VTMCD, resonance Raman, Mössbauer, and redox studies of wild-type, NEM-modified, C57S, and C87A *Synechocystis* FTR as well as the *Synechocystis* FTR/Trx *m* heterodisulfide complex. The results confirm the proposal of distinct and noninterchangeable roles for the active-site cysteines and the formation of an FTR/Trx heterodisulfide complex that is a potential analogue of a one-electron-reduced catalytic intermediate, with spectroscopic and redox properties similar to those of oxidized NEM-FTR. In addition, the Mössbauer studies reveal novel site-specific $[Fe_4S_4]$ cluster chemistry in all three redox states of FTR (oxidized, one-electron-reduced, and two-electron-reduced) and raise the possibility of an alternative mechanism in which FTR is reduced by two electrons prior to interaction with Trx.

(10) Staples, C. R.; Gaymard, E.; Stritt-Etter, A.-L.; Telser, J.; Hoffman, B. M.; Schürmann, P.; Knaff, D. B.; Johnson, M. K. *Biochemistry* **1998**, *37*, 4612−4620.
(11) Jameson, G. N. L.; Walters, E. M.; Manieri, W.; Schürmann, P.; Johnson, M. K.; Huynh, B. H. *J. Am. Chem. Soc.* **2003**, *125*, 1146−1147.
(12) Walters, E. M.; Johnson, M. K. *Photosynth. Res.* **2004**, *79*, 249−264.
(13) Glauser, D. A.; Bourquin, F.; Manieri, W.; Schürmann, P. *J. Biol. Chem.* **2004**, *279*, 16662−16669.

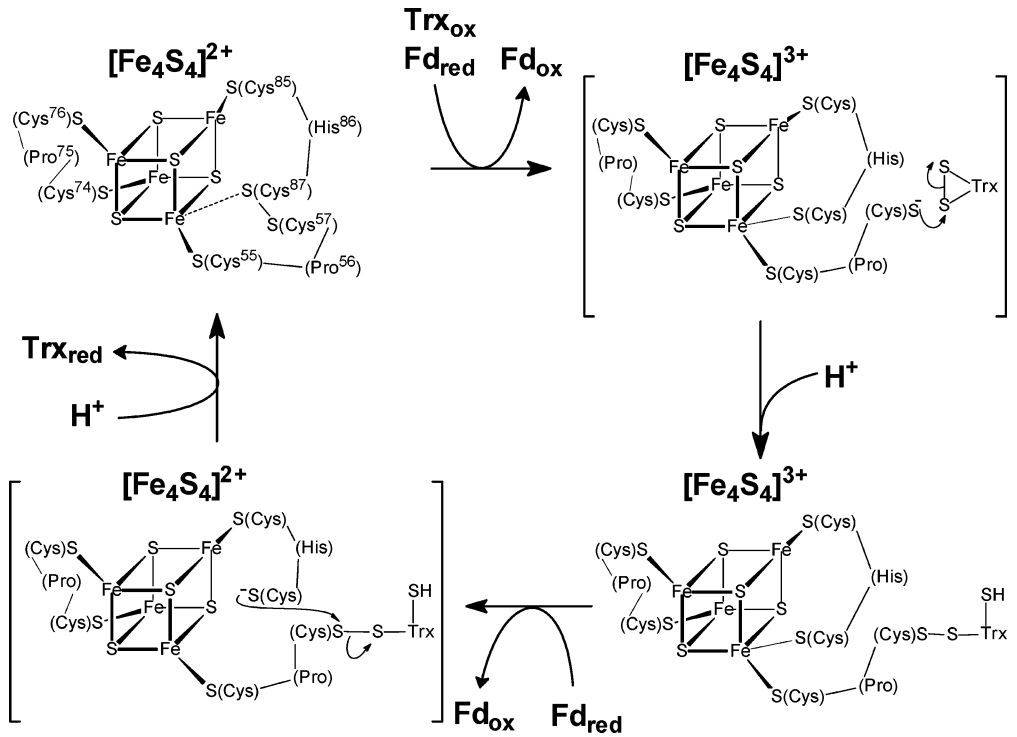

Figure 2. Proposed catalytic mechanism for FTR.[12] Residue numbering is for *Synechocystis* FTR. Square brackets are used to indicate transient intermediates.

Experimental Methods

Protein Expression and Purification. The construction of the overexpression strains as well as the procedures used for overexpression and purification of wild-type, C87A, and C57S *Synechocystis* FTR, wild-type spinach FTR, and the C40S variant of spinach Trx *m* have been described elsewhere.[13,14] Incorporation of ^{57}Fe for Mössbauer analysis was effected by addition of ^{57}Fe ferric ammonium citrate to chelex-resin-treated LB media to a final Fe concentration of 5 mg/L.[11]

Sample Preparation and Handling. Recombinant wild-type spinach and *Synechocystis* FTR were initially purified with varying amounts of the enzyme in a form that closely resembles NEM-FTR based on EPR studies (up to 20% based on EPR spin quantitations). The EPR-silent oxidized form of recombinant FTR was generally obtained only after redox cycling the enzyme by dithionite reduction followed by O_2 oxidation. This redox-cycled form of oxidized wild-type FTR was used as the starting material for the formation of methyl viologen reduced FTR, NEM-FTR, and the heterodisulfide complex between FTR and C40S Trx *m*. The formation of the heterodisulfide complex was performed as described elsewhere.[13] Both C87A and C57S FTR were used in the as-purified form, and spectroscopic studies gave no indication of heterogeneity in the vicinity of the $[Fe_4S_4]^{2+}$ cluster. Unless otherwise indicated, all forms of FTR were in 20 mM triethanolamine-HCl buffer, pH 7.3, and were handled under anaerobic conditions in a Vacuum Atmospheres glovebox under an Ar atmosphere (<1 ppm O_2).

Selective NEM modification of Cys57 of WT FTR to form NEM-FTR was carried out by reducing FTR under anaerobic conditions with a 3-fold excess of reduced methyl viologen, incubating for 30 min to ensure complete reduction of the active-site disulfide, followed by cooling on ice for 10 min and treating with a 5-fold excess of NEM for 2 min prior to quenching the reaction by exposure to air. Excess reagents were removed by gel-filtration, and the sample was concentrated by Amicon ultrafiltration using a YM10 membrane. Sample concentrations were based upon $\epsilon_{410} = 17\,400\ M^{-1}\ cm^{-1}$ for WT and C87A FTR, and $\epsilon_{410} = 19\,500\ M^{-1}\ cm^{-1}$ for NEM-FTR, C57S FTR, and the FTR/C40S Trx *m* heterodisulfide complex.[13,15,16]

Dye-mediated redox titrations were performed on NEM-FTR and the FTR/C40S Trx *m* heterodisulfide complex at ambient temperature (25−27 °C) in a Vacuum Atmospheres glovebox under argon (<1 ppm O_2). The pH dependence of the midpoint redox potential was determined using enzyme in a buffer cocktail containing 200 mM MES, MOPS, and TAPS buffers, which allows for easy variation of the pH in the desired range (6.0−8.5). Mediator dyes were added, each to a final concentration of 50 μM, to cover the desired range of redox potentials, that is, methyl viologen, benzyl viologen, neutral red, safranin, phenosafranin, anthroquinone-1,5-disulfonate, indigodisulfonate, methylene blue, 1,2-naphthoquinone, duroquinone, and 1,2-naphthoquinone-4-sulfonate. The starting point of the titrations was the oxidized as-prepared sample, and the potential was poised by reductive titration using 10 mM dithionite in the redox titration buffer at the same pH as the protein titration mixture. Upon completion of the reductive titration, 10 mM potassium ferricyanide in the same redox titration buffer was added to return the potential to a value approximately that of the starting material to test whether the reduction was reversible and to access the extent of reoxidation. For all data points, a 0.25-mL aliquot was transferred to an EPR tube after equilibration at the desired potential, and the sample was immediately frozen in liquid nitrogen. Potentials were measured with a platinum working electrode and a saturated calomel reference electrode and are reported relative to NHE. All redox titration data have been normalized for dilution effects that occur throughout the reduction titration. To assess if cleavage of the FTR/C40S Trx *m* heterodisulfide occurs concomitant with the EPR-monitored reduction of the complex, samples poised at selected potentials were removed and loaded onto a 5-mL High-Performance Q-Sepharose column under strictly anaerobic conditions inside the glovebox. A linear gradient from 0.0 to 0.5 M NaCl in 20 mM triethanolamine-HCl, pH 7.3 buffer was used to elute the components and separate the FTR/Trx *m* complex from free C40S Trx *m* and wild-type FTR. The components

(14) Gaymard, E.; Franchini, L.; Manieri, W.; Stutz, E.; Schürmann, P. *Plant Sci.* **2000**, *158*, 107−113.

(15) Droux, M.; Jacquot, J.-P.; Miginac-Maslow, M.; Gadal, P.; Huet, J. C.; Crawford, N. A.; Yee, B. C.; Buchanan, B. B. *Arch. Biochem. Biophys.* **1987**, *252*, 426−439.

(16) Schürmann, P.; Gardet-Salvi, L. *Chimia* **1993**, *47*, 245−246.

in the elution profile were identified by parallel studies of the elution profiles of the oxidized FTR/Trx *m* complex, C40S Trx *m*, and wild-type FTR.

Spectroscopic Measurements. X-band (~9.6 GHz) EPR spectra were recorded on a Bruker ESP300E spectrometer equipped with an ER-4116 dual mode cavity and an Oxford Instruments ESR-9 flow cryostat. Raman spectra were recorded with an Instruments SA U1000 spectrometer fitted with a cooled RCA 31034 photomultiplier tube, using 457-nm excitation from a Coherent Innova 10-W Ar^+ laser. Scattering was collected at 90° from the surface of a frozen 15 μL droplet of protein in a specially constructed anaerobic cell mounted on the coldfinger of an Air Products Displex model CSA-202E closed cycle refrigerator.[17] The spectrum of the frozen buffer solution, normalized to the intensity of the ice-band at 230 cm^{-1}, has been subtracted from all of the spectra shown in this work. Variable-temperature magnetic circular dichroism (VTMCD) measurements were carried out with an Oxford Instruments Spectromag 4000 split-coil superconducting magnet mated to a Jasco J715 spectropolarimeter using the published protocols.[18,19] Mössbauer spectra were recorded using the previously described spectrometers.[20] The zero velocity refers to the centroid of the room-temperature spectra of metallic iron foil. Analysis of the Mössbauer data was performed with the program WMOSS (WEB Research).

Results

Previous spectroscopic investigations on FTR have concentrated on the oxidized and NEM-modified forms of the native and recombinant forms of the spinach enzyme.[8,10,11] In this manuscript, the emphasis is on spectroscopic characterization of crystallographically defined recombinant FTR from *Synechocystis* and selected site-specific variants, in each of their accessible redox states. Spectroscopic data of oxidized and NEM-modified *Synechocystis* FTR will also be presented for the purposes of establishing the commonality between the spinach and *Synechocystis* enzymes, and for providing references for comparison studies with those of the other forms of FTR that are characterized in this work.

Oxidized FTR. Figure 3 shows the 4.2-K Mössbauer spectra of oxidized recombinant *Synechocystis* FTR recorded in a weak magnetic field of 50 mT (A) and a strong field of 6 T (B) applied parallel to the γ beam. The presence of a unique Fe site in the $[Fe_4S_4]$ cluster is readily observable as a prominent shoulder on the side of the high energy line of both spectra. Similar to oxidized recombinant spinach FTR,[11] these spectra can be interpreted as superpositions of three spectral components with an intensity ratio of 1:1:2, corresponding to three distinct Fe sites, *a*, *b*, and *c* (Table 1), arising from the diamagnetic $S = 0$ ground state of a $[Fe_4S_4]^{2+}$ cluster. Within experimental errors, the parameters obtained for *Synechocystis* FTR (Table 1) are identical to those reported for spinach FTR.[11] Sites *b* and *c* exhibit parameters within the ranges observed for typical $[Fe_4S_4]^{2+}$ clusters and thus represent Fe sites of regular coordination (i.e., tetrahedral S coordination) and oxidation state ($Fe^{2.5+}$) that are expected for a $[Fe_4S_4]^{2+}$ cluster.[21−24] The doubled absorption intensity determined for site *c* indicates further that it represents a valence-delocalized $Fe^{2+}Fe^{3+}$ pair

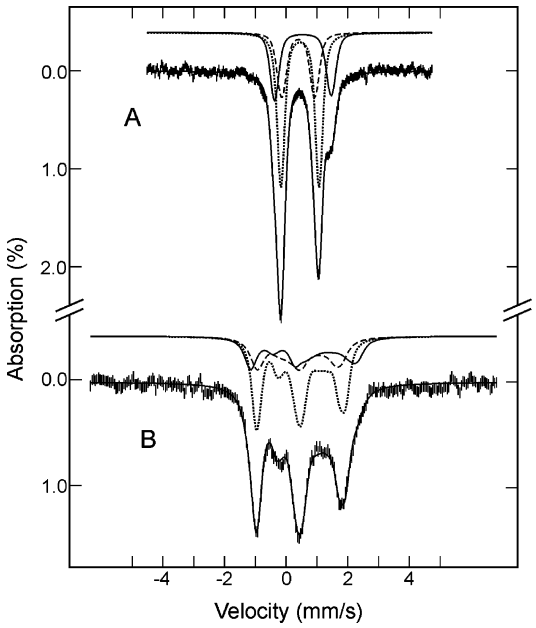

Figure 3. Mössbauer spectra of oxidized wild-type *Synechocystis* FTR. The data (hatched marks) were recorded at 4.2 K in a magnetic field of 50 mT (A) or 6 T (B) applied parallel to the γ-radiation. The solid lines overlaid with the experimental spectra are least-squares fits to the data using three quadrupole doublets with an intensity ratio of 1:1:2 representing three Fe sites *a*, *b*, and *c* (see text and Table 1). The spectra representing the individual Fe sites are shown above the experimental spectra as solid lines (site *a*), dashed lines (site *b*), and dotted lines (site *c*).

within the cluster. Site *a*, however, with its larger δ and ΔE_Q, represents a unique Fe site with atypical coordination environment. Based on the X-ray crystallographic structure determined for *Synechocystis* FTR,[9] site *a* is assigned to the Fe atom coordinated to residue C55 (C52 for spinach FTR). This Fe atom and the coordinated cysteinyl-S atom are in van der Waals contact (3.1 Å) with one of the S atoms that form the active-site disulfide (C57 and C87), see Figure 1, resulting in an iron site having a distorted tetrahedral coordination,[9,11,12] and thus increased ΔE_Q. We have suggested that this interaction between the unique Fe and the active-site disulfide is of mechanistic importance:[11] It promotes charge buildup at the unique Fe site (and therefore the increased δ value), making it an electron donor, and polarizes the disulfide bond, making the interacting S of C87 an electron acceptor. The resting enzyme is therefore primed to accept an electron for the breaking of the disulfide bond.

The resonance Raman spectrum of the oxidized recombinant *Synechocystis* FTR (Figure 4A) is very similar to that reported and assigned for the native spinach enzyme as purified,[8] and the frequencies and relative intensities of the bands are characteristic of $[Fe_4S_4]^{2+}$ clusters with complete cysteinyl-S coordination.[25] Weak interaction between the unique Fe site and the disulfide is not readily apparent in the resonance Raman spectrum. However, as discussed below, interaction with the

(17) Drozdzewski, P. M.; Johnson, M. K. *Appl. Spectrosc.* **1988**, *42*, 1575−1577.
(18) Johnson, M. K. In *Metal clusters in proteins*; Que, L., Jr., Ed.; American Chemical Society: Washington, DC, 1988; pp 326−342.
(19) Thomson, A. J.; Cheesman, M. R.; George, S. J. *Methods Enzymol.* **1993**, *226*, 199−232.
(20) Ravi, N.; Bollinger, J. M.; Huynh, B. H.; Edmondson, D. E.; Stubbe, J. *J. Am. Chem. Soc.* **1994**, *116*, 8007−8014.
(21) Middleton, P.; Dickson, D. P. E.; Johnson, C. E.; Rush, J. D. *Eur. J. Biochem.* **1978**, *88*, 135−141.
(22) Tong, W.-H.; Jameson, G. N. L.; Huynh, B. H.; Rouault, T. A. *Proc. Natl. Acad. Sci. U.S.A.* **2003**, *100*, 9762−9767.
(23) Trautwein, A. X.; Bill, E.; Bominaar, E. L.; Winkler, H. *Struct. Bonding* **1991**, *78*, 1−95.
(24) Yoo, S. J.; Angove, H. C.; Burgess, B. K.; Hendrich, M. P.; Münck, E. *J. Am. Chem. Soc.* **1999**, *121*, 2534−2545.
(25) Conover, R. C.; Kowal, A. T.; Fu, W.; Park, J.-B.; Aono, S.; Adams, M. W. W.; Johnson, M. K. *J. Biol. Chem.* **1990**, *265*, 8533−8541.

Table 1. Mössbauer Parameters of Various Forms of Ferredoxin:Thioredoxin Reductases from *Synechocystis* and Spinach[a]

cluster state	protein	Fe site	δ (mm/s)	ΔE_Q (mm/s)	η	$A_{xx}/g_n\beta_n$ (T)	$A_{yy}/g_n\beta_n$ (T)	$A_{zz}/g_n\beta_n$ (T)
$[Fe_4S_4]^{2+}$	oxidized	a	0.54 (2)	1.84 (3)	0.0			
$S = 0$	*Syn.* FTR	b	0.39 (2)	1.07 (3)	0.5			
		c	0.45 (2)	1.24 (3)	0.5			
	Syn. C87A FTR	a	0.51 (2)	1.65 (3)				
		b	0.43 (2)	1.05 (3)				
		c	0.43 (2)	1.27 (3)				
	reduced *Syn.*	a	0.67 (2)	2.52 (3)	0.0			
	C57S FTR	b	0.35 (2)	1.00 (3)	0.9			
		c	0.49 (2)	1.12 (3)	0.8			
	MV-reduced	a	0.69 (2)	2.58 (3)				
	spinach FTR	b	0.35 (2)	1.00 (3)				
		c	0.49 (2)	1.13 (3)				
$[Fe_4S_4]^{3+}$	oxidized *Syn.*	a	0.32	1.2	0.3	20.5 (2.0)	20.5 (2.0)	8.0 (2.0)
$S = 1/2$	NEM-FTR[b]	b	0.29	−0.9	0.5	22.0 (1.0)	22.0 (1.0)	19.5 (2.0)
		c	0.45	1.2	0.0	−30.0 (1.0)	−25.0 (1.0)	−25.0 (1.0)

[a] Values in parentheses indicate uncertainties in the last digits. [b] The electronic relaxation rate of NEM-FTR at high temperatures (above 200 K) is comparable to the ^{57}Fe nuclear precession rate, resulting in an extremely broad, asymmetric, and poorly defined doublet. This has prevented us from obtaining an accurate measure of the ΔE_Q and δ values. In the analysis, the ΔE_Q values were restricted within a range (0.8−1.2 mm/s) that is not in conflict with the high-temperature data. To further reduce the number of parameters, the magnetic hyperfine A tensors for the three Fe sites were assumed to be axial. With these assumptions, the uncertainties for the δ values were estimated to be ±0.02 mm/s. The uncertainties of the A values were estimated by varying each A value separately while keeping all other parameters fixed.

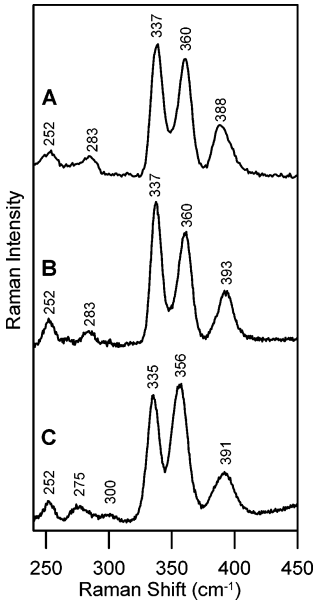

Figure 4. Comparison of the resonance Raman spectra of $[Fe_4S_4]^{2+}$ centers in wild-type, C57S, and C87A *Synechocystis* FTR: (A) Oxidized wild-type FTR; (B) as purified C87A FTR; (C) dithionite-reduced C57S FTR. All samples were ∼3 mM in FTR, and all spectra were recorded at 17 K using 457.9-nm laser excitation with ∼200 mW laser power at the sample. Each scan involved photon counting for 1 s at 1 cm^{-1} increments with 7 cm^{-1} bandwidth, and each spectrum is the sum of 80−100 scans. For all spectra, the vibrational modes originating from the frozen buffer solution have been subtracted after normalizing the intensities of the "ice-band" at 231 cm^{-1}.

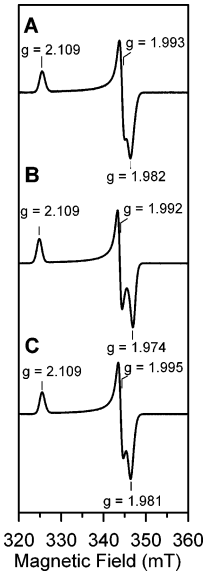

Figure 5. Comparison of the X-band EPR spectra of $[Fe_4S_4]^{3+}$ centers in the oxidized (as purified) forms of *Synechocystis* FTR samples: (A) NEM-FTR (185 μM); (B) wild-type FTR/C40S Trx *m* heterodisulfide complex (95 μM); (C) C57S FTR (255 μM). EPR conditions: temperature, 35 K; microwave power, 1 mW; modulation amplitude, 0.63 mT; microwave frequency, 9.60 GHz.

disulfide is suggested by changes in the resonance Raman spectra of the $[Fe_4S_4]^{2+}$ center in oxidized FTR as compared to the spectra of the $[Fe_4S_4]^{2+}$ centers in the as-purified C87A variant and dithionite-reduced C57S variant, see Figure 4.

Oxidized NEM-FTR. One of the cysteine residues forming the active-site disulfide (Cys54 in spinach FTR and Cys57 in *Synechocystis* FTR) becomes solvent exposed on reduction and hence can be selectively alkylated by NEM in methyl viologen-reduced FTR, resulting in the formation of NEM-FTR. In contrast to oxidized wild-type FTR, which is EPR silent, NEM-FTR shows an intense near-axial $S = 1/2$ EPR signal in the oxidized (as-purified) form.[8,10] Figure 5A shows the 35-K EPR spectrum of oxidized *Synechocystis* NEM-FTR, which comprises a near-axial resonance with $g = 2.11$, 1.99, and 1.98. Very similar EPR signals have been reported for the oxidized NEM-modified form of native spinach FTR,[8,10] and in both the resonances account for approximately 1 spin/FTR and can be observed up to 150 K without significant broadening.

The observations that oxidized NEM-FTR exhibits an EPR signal with an average g value larger than 2.0 and that one-electron reduction converts the $S = 1/2$ EPR-active NEM-FTR into an EPR-silent form with a $S = 0$ $[Fe_4S_4]^{2+}$ cluster[8] are consistent with NEM-FTR containing a $[Fe_4S_4]^{3+,2+}$ cluster. Moreover, optical absorption, resonance Raman, ENDOR, VTMCD, and Mössbauer spectroscopies[8,10,11] have been used to characterize oxidized spinach NEM-FTR, and the results unambiguously confirmed the presence of a $[Fe_4S_4]^{3+}$ cluster. The VTMCD spectra of oxidized *Synechocystis* NEM-FTR

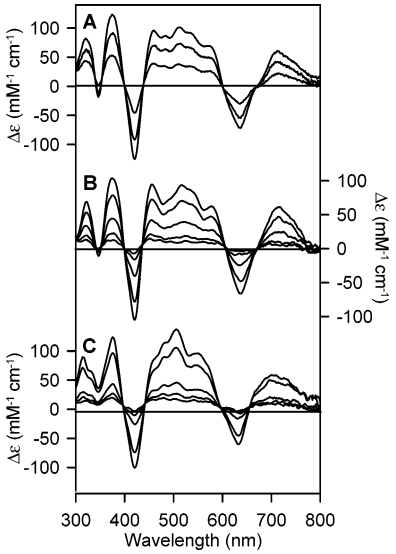

Figure 6. Comparison of the VTMCD spectra of $[Fe_4S_4]^{3+}$ centers in the oxidized (as purified) forms of *Synechocystis* FTR samples. (A) MCD spectra of NEM-FTR collected at 1.68, 4.22, and 10.4 K, with a magnetic field of 6 T. (B) MCD spectra of wild-type FTR/C40S Trx *m* heterodisulfide complex collected at 1.68 , 4.22, 10.4, 25, and 50 K, with a magnetic field of 6 T. (C) MCD spectra of C57S FTR collected at 1.68, 4.22, 10.4, 25, and 50 K, with a magnetic field of 6 T. For all spectra, the intensity of all MCD bands (positive and negative) increases with decreasing temperature.

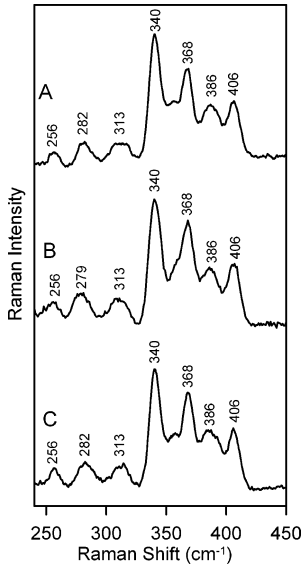

Figure 7. Comparison of the resonance Raman spectra of $[Fe_4S_4]^{3+}$ centers in the oxidized (as purified) forms of *Synechocystis* FTR samples: (A) NEM-FTR, (B) wild-type FTR/C40S Trx *m* heterodisulfide complex, and (C) C57S FTR. All samples were ~3 mM in FTR, and all spectra were recorded at 17 K using 457.9-nm laser excitation with ~175 mW laser power at the sample. Each scan involved photon counting for 1 s at 1 cm^{-1} increments with 7 cm^{-1} bandwidth, and each spectrum is the sum of 70−100 scans. For all spectra, the vibrational modes originating from the frozen buffer solution have been subtracted after normalizing the intensities of the "ice-band" at 231 cm^{-1}.

(Figure 6A) are very similar to those observed for the spinach enzyme[8] and show saturation magnetization behavior consistent with transitions originating from a $S = {}^1/_2$ ground state, indicating that both the EPR and the VTMCD transitions are arising from the same paramagnetic ground state. The complex and intense pattern of VTMCD bands observed for oxidized NEM-FTR can only be interpreted in terms of the unpaired spin being associated with a $[Fe_4S_4]^{3+}$ cluster. However, the VTMCD spectra are quite distinct from those observed for $[Fe_4S_4]^{3+}$ clusters in high-potential iron−sulfur proteins (HiPIPs),[26] suggesting some unique excited-state electronic properties for this type of $[Fe_4S_4]^{3+}$ center. The resonance Raman spectrum of oxidized *Synechocystis* NEM-FTR (Figure 7A) is also very similar to that reported and assigned for oxidized spinach NEM-FTR.[8] Furthermore, the changes in the resonance Raman spectrum of oxidized *Synechocystis* NEM-FTR as compared to that of the $[Fe_4S_4]^{2+}$ center in oxidized *Synechocystis* FTR (cf. Figures 7A and 4A), that is, small upshifts ($\leq$3 cm^{-1}) in most of the predominantly bridging Fe−S stretching modes and large upshifts ($\leq$17 cm^{-1}) in all of the predominantly terminal Fe−S(Cys) stretching modes, are consistent with the presence of a $[Fe_4S_4]^{3+}$ cluster in oxidized NEM-FTR. Nevertheless, the resonance Raman spectrum of NEM-FTR shows significant differences, as compared to those reported for $[Fe_4S_4]^{3+}$ centers in HiPIPs,[27,28] suggesting some unique structural properties for this type of $[Fe_4S_4]^{3+}$ center. In addition, there are intriguing differences in the redox and ground-state electronic properties for the $[Fe_4S_4]^{3+}$ cluster in oxidized NEM-FTR as compared to those in HiPIPs.[8,10] In particular, the midpoint potential for the $[Fe_4S_4]^{3+,2+}$ couple is at least 500 mV lower, and the ground-state spin relaxation rate for the $S = {}^1/_2$ $[Fe_4S_4]^{3+}$ center is much slower. The difference in spin relaxation is manifest by the ability to observe the EPR signal at 150 K without broadening for oxidized NEM-FTR samples, whereas the oxidized HiPIP EPR signals can only be observed at a temperature below 30 K.[29] These differences suggest a new-type of $[Fe_4S_4]^{3+}$ cluster in NEM-FTR.

In oxidized NEM-FTR, the active-site disulfide bond has been cleaved by a two-electron reduction, and, as indicated by the above-mentioned spectroscopic data, the $[Fe_4S_4]$ cluster is in the 3+ state. Consequently, oxidized NEM-FTR is one-electron more reduced than the resting enzyme. Previous investigations have shown that $S = {}^1/_2$ EPR signals analogous to that of oxidized NEM-FTR were observed as transient species in spinach FTR during catalytic turnover and during reduction with substoichiometric amounts of reducing agent.[10] On the basis of these observations, it has been suggested that NEM-FTR provides a stable analogue of a one-electron-reduced catalytic intermediate in the enzymatic cycle.[10] Furthermore, the difference in solvent accessibility of the two thiols of the active-site disulfide has led to the proposal that the more exposed thiol (Cys57 in *Synechocystis*), termed the interchange thiol, is responsible for attacking the substrate disulfide, while the less exposed thiol (Cys87 in *Synechocystis*), termed the cluster-interacting thiol, interacts with the nearby $[Fe_4S_4]$ cluster, resulting in a novel cluster with five cysteine ligands. The observed anomalous structural, electronic, and redox properties for the $[Fe_4S_4]^{3+}$ center in oxidized NEM-FTR were thus attributed to coordination of the cluster-interacting cysteine, Cys87, to the Fe_4S_4 cluster.[10] The binding site for the fifth

(26) Johnson, M. K.; Robinson, A. E.; Thomson, A. J. In *Iron−sulfur proteins*, 1st ed.; Spiro, T. G., Ed.; Wiley−Interscience: New York, 1982; pp 367−406.
(27) Czernuszewicz, R. S.; Macor, K. A.; Johnson, M. K.; Gewirth, A.; Spiro, T. G. *J. Am. Chem. Soc.* **1987**, *109*, 7178−7187.
(28) Backes, G.; Mino, Y.; Loehr, T. M.; Meyer, T. E.; Cusanovich, M. A.; Sweeney, W. V.; Adman, E. T.; Sanders-Loehr, J. *J. Am. Chem. Soc.* **1991**, *113*, 2055−2064.
(29) Dunham, W. R.; Hagen, W. R.; Fee, J. A.; Sands, R. H.; Dunbar, J. B.; Humblet, C. *Biochim. Biophys. Acta* **1991**, *1079*, 253−262.

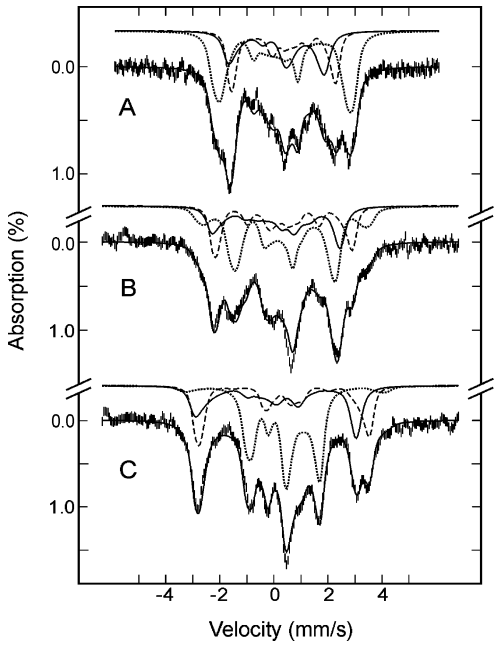

Figure 8. 4.2-K Mössbauer spectra of oxidized *Synechocystis* NEM-FTR recorded in a parallel field of 50 mT (A), 4 T (B), and 8 T (C). The data (hatched marks) can be decomposed into three components with an intensity ratio of 1:1:2 representing two distinct ferric sites (sites *a* and *b*) and a valence-delocalized $Fe^{2+}Fe^{3+}$ pair (site *c*). An $S = {}^1/_2$ ground state is assumed for the analysis. The theoretical spectra corresponding to the three components are shown above the experimental spectra as solid lines (site *a*), dashed lines (site *b*), and dotted lines (site *c*). The sums of the three components are plotted as solid lines overlaid with the experimental spectra. The parameters used for the simulation are listed in Table 1. This NEM-reacted sample contains approximately 12% methyl viologen-reduced FTR (starting materials). For clarity, the contribution from the reduced FTR has been removed from the raw data using spectra simulated with parameters listed in Table 1 for the reduced FTR-C57S.

cysteine ligand, however, was not identified. More recently, our initial Mössbauer characterization of the spinach FTR has confirmed the binding of a fifth cysteine ligand to the $[Fe_4S_4]^{3+}$ cluster in oxidized NEM-FTR.[11] Furthermore, due to the ability of Mössbauer spectroscopy to differentiate and detect individual Fe sites within a cluster, the fifth cysteine coordination site was revealed to be the unique Fe site *a*. Here, a more detailed Mössbauer study of the *Synechocystis* NEM-FTR is presented.

At 4.2-K, oxidized *Synechocystis* NEM-FTR exhibits magnetic field-dependent Mössbauer spectra (Figure 8) that are consistent with a paramagnetic $S = {}^1/_2$ electronic ground state. These spectra are very similar to those observed for oxidized spinach NEM-FTR[11] and, as reported for the spectra of the spinach enzyme, can also be decomposed into three components with an intensity ratio of 1:1:2. This intensity ratio, together with the parameters (Table 1) determined for the components, indicate a cluster composed of two ferric sites (sites *a* and *b*) and a valence-delocalized $Fe^{2+}Fe^{3+}$ pair (site *c*), consistent with the $[Fe_4S_4]^{3+}$ assignment. The magnitudes and signs of the magnetic-hyperfine *A* tensors compare well with those of the $[Fe_4S_4]^{3+}$ cluster in HiPIP.[30,31] The opposite signs of the *A* tensors reflect the antiparallel orientations between the spin of the mixed-valence pair and the spins of the two ferric sites. A major difference observed between the $[Fe_4S_4]^{3+}$ clusters in HiPIP and in NEM-FTR is that the two ferric ions are indistinguishable in HiPIP, but they are distinct in NEM-FTR. This distinction between the two ferric sites is most obvious in the 8-T spectrum (Figure 8C) in which the corresponding spectral components, *a* and *b*, are clearly resolved in the region between +3 and +4 mm/s. Moreover, our detailed analysis of these field-dependent spectra yielded different δ values for the two ferric sites (Table 1). While the smaller δ value, 0.29 mm/s, determined for site *b* is consistent with ferric sites with tetrahedral sulfur coordination,[32,33] the larger δ value, 0.32 mm/s, determined for site *a* suggests a ferric site with a higher coordination number, consistent with binding of a fifth ligand at this site. A comparison of the parameters of NEM-FTR with those of the as-purified FTR shows that, while there are practically no changes observed for the ΔE_Q and δ values for site *c*, significant reductions in the δ values are observed for sites *a* and *b*, indicating that oxidation of the cluster occurs at these two Fe sites. The larger reduction of δ observed for site *a* (0.54 to 0.32 mm/s) further indicates that most of the reducing equivalent is removed from this unique Fe site *a*. Consequently, the Mössbauer data not only confirm the 3+ oxidation state of the $[Fe_4S_4]$ cluster in NEM-FTR, the data also reveal detailed electronic and structural changes at the $[Fe_4S_4]$ cluster upon NEM-modification. That is, the unique Fe site, identified in the as-purified FTR, retains its distinctiveness in the NEM-FTR complex, in which alkylation of Cys57 results in coordination of Cys87 to the unique Fe site and oxidation of the cluster. Moreover, the unique Fe site provides most of the reducing equivalent removed from the cluster.

Wild-Type FTR/C40S Trx *m* Heterodisulfide Complex. Recently, a detailed investigation of the interactions of wild-type and site-specific variants of *Synechocystis* FTR with spinach Trx *m* and *f* has shown that stable FTR/Trx heterodisulfide complexes can be formed using active-site modified Trxs.[13] These complexes are analogues of a potential catalytic intermediate (see Figure 2) and have been shown to exhibit optical spectra indicative of an oxidized $[Fe_4S_4]^{3+}$ cluster in the oxidized (as purified) form. To further investigate the structural and electronic properties of the $[Fe_4S_4]$ cluster in FTR/Trx heterodisulfide complexes, we report here a detailed spectroscopic characterization of the FTR/Trx heterodisulfide complex formed with wild-type *Synechocystis* FTR and spinach C40S Trx *m*.

Figure 5B shows the 35-K EPR spectrum of the FTR/C40S Trx *m* heterodisulfide complex. The spectrum is very similar to that of NEM-FTR shown in Figure 5A and exhibits a near-axial $S = {}^1/_2$ EPR signal with $g = 2.11$, 1.99, and 1.97. This signal accounts for approximately 1 spin per molecule of the complex. As mentioned above, the $[Fe_4S_4]^{3+}$ cluster in NEM-FTR displays atypical electronic relaxation behavor that allows its EPR signal to be observed up to 150 K. Similarly, the EPR signal of the FTR/Trx *m* complex can also be observed up to 150 K without significant broadening. The VTMCD spectrum of the heterodisulfide complex (Figure 6B) displays a complex pattern of temperature-dependent bands that is very similar to that of oxidized NEM-FTR (Figure 6A) and exhibits similar temperature and magnetic-field dependence. Not surprisingly,

(30) Bertini, I.; Campos, A. P.; Luchinat, C.; Teixeira, M. *J. Inorg. Biochem.* **1993**, *52*, 227−234.
(31) Middleton, P.; Dickson, D. P. E.; Johnson, C. E.; Rush, J. D. *Eur. J. Biochem.* **1980**, *104*, 289−296.
(32) Moura, I.; Huynh, B. H.; Hausinger, R. P.; LeGall, J.; Xavier, A. V.; Münck, E. *J. Biol. Chem.* **1980**, *255*, 2493−2498.
(33) Yoo, S. J.; Meyer, J.; Achim, C.; Peterson, J.; Hendrich, M. P.; Münck, E. *J. Biol. Inorg. Chem.* **2000**, *5*, 475−487.

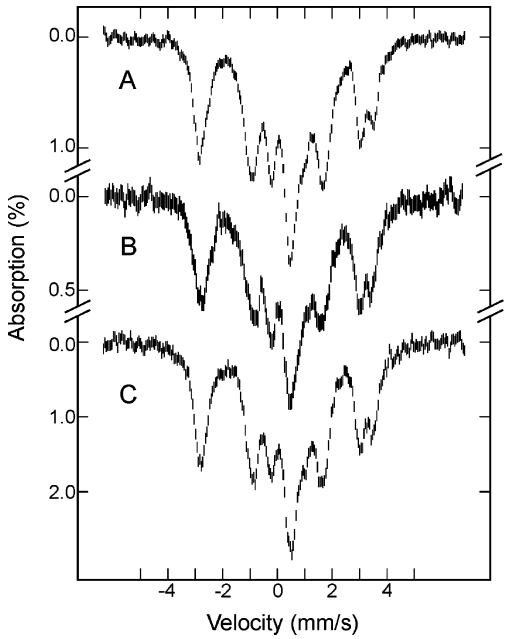

Figure 9. Comparison of the Mössbauer spectra of $[Fe_4S_4]^{3+}$ centers in the oxidized (as purified) forms of *Synechocystis* FTR samples: (A) NEM-FTR; (B) wild-type FTR/C40S Trx *m* heterodisulfide complex; (C) C57S FTR. The spectra were recorded at 4.2 K in a parallel field of 8 T.

the resonance Raman spectrum of the FTR/Trx heterodisulfide complex (Figure 7B) also shows Raman bands that are very similar to those detected for NEM-FTR (Figure 7A), in both intensities and frequencies. To further establish the similarities between the clusters in oxidized NEM-FTR and in FTR/C40S Trx *m* heterodisulfide complex, Mössbauer spectra of the heterodisulfide complex were recorded over a wide range of magnetic fields (50 mT to 8 T) for a detailed characterization of the distinguishable Fe sites present in the cluster of the heterodisulfide complex. Within experimental uncertainties, the field-dependent Mössbauer spectra of the heterodisulfide complex were found to be identical to those of NEM-FTR. Because the spectra of the three distinct Fe sites (*a*, *b*, and *c*) are best resolved in an applied field of 8 T, we present, in Figure 9, the 4.2-K 8-T Mössbauer spectrum of the heterodisulfide complex (Figure 9B) in comparison with the corresponding spectrum of NEM-FTR (Figure 9A). Clearly, it can be seen that the two spectra are identical. Thus, the overwhelming spectroscopic evidence presented here has firmly established that the electronic structures of the $[Fe_4S_4]$ cluster in oxidized NEM-FTR and in the FTR/C40S Trx *m* heterodisulfide complex are identical, strongly supporting the suggestion that NEM-FTR represents a stable analogue of the one-electron-reduced FTR/Trx heterodisulfide complex in the proposed mechanistic pathway (Figure 2).

C57S and C87A Variants of *Synechocystis* FTR. To obtain further information on the specific roles played by the two cysteine residues of the active-site disulfide, site-specific *Synechocystis* FTR variants of these two residues (Cys57 and Cys87) have been expressed in *E. coli*, purified, and characterized by a variety of biochemical methods and UV−vis absorption spectroscopy.[13] Substitutions at either Cys57 or Cys87 result in inactive enzymes, establishing that both residues are essential for FTR function.[13] In accord with distinct roles for each of the two active-site cysteines, the oxidized (as purified) forms of the C87A and C57S variants were found to exhibit UV−vis absorption spectra typical of $[Fe_4S_4]^{2+}$ and $[Fe_4S_4]^{3+}$ centers, respectively.[13] Here, we present the resonance Raman spectrum, the 35-K EPR spectrum, the VTMCD spectra, and the 4.2-K 8-T Mössbauer spectrum of oxidized *Synechocystis* C57S FTR, respectively, in Figures 5C, 6C, 7C, and 9C for comparison with the corresponding spectra of the oxidized *Synechocystis* NEM-FTR and the wild-type *Synechocystis* FTR/C40S Trx *m* heterodisulfide complex. It is plainly apparent that the spectroscopic data of these three forms of FTR are almost indistinguishable, indicating strongly that the electronic structures of the $[Fe_4S_4]$ clusters in all three proteins are identical. In other words, oxidized C57S FTR also contains a novel five-cysteine coordinated $[Fe_4S_4]^{3+}$ cluster with a unique five-coordinate Fe site. Thus, the spectroscopic data demonstrate that substitution of the interchange thiol, Cys57, frees the cluster-interacting thiol, Cys87, to react with the $[Fe_4S_4]$ cluster and results in coordination of Cys87 to the unique Fe site *a* in the oxidized state. These data provide strong support for the detailed mechanism proposed for the interaction between Cys87 and the $[Fe_4S_4]$ cluster.[11]

In accord with the UV−vis absorption spectroscopy,[13] the resonance Raman spectrum of *Synechocystis* C87A FTR as purified (Figure 4B) shows vibrational bands indicative of $[Fe_4S_4]^{2+}$ cluster. The spectrum is very similar to that of oxidized *Synechocystis* FTR (Figure 4A), and the only significant difference lies in a 5-cm^{-1} upshift in the highest frequency Fe−S stretching band, which is centered at 393 cm^{-1} in the C87A variant. This band is broad due to the overlap of two Fe−S stretching modes, an asymmetric stretching mode of the Fe_4S_4 core and the symmetric Fe−S(Cys) stretching mode,[8] and the change in frequency is likely to reflect greater resonance enhancement of the higher energy symmetric Fe−S(Cys) stretching mode. This would be consistent with more symmetrical cluster ligation in the C87A variant due to loss of the interaction with active-site disulfide. However, the identical frequencies for the Fe−S stretching modes of the $[Fe_4S_4]^{2+}$ core in wild-type and C87A FTR (asymmetric modes at 252 and 283 cm^{-1} and symmetic (breathing) mode at 337 cm^{-1}) indicate that loss of the active-site disulfide has no significant effect on the structure of the Fe_4S_4 core.

The Mössbauer spectrum of C87A FTR recorded at 4.2 K in a weak magnetic field of 50 mT (Figure 10) shows a nearly symmetric quadrupole doublet with apparent parameters (ΔE_Q = 1.33 mm/s and δ = 0.45 mm/s) that are characteristic of $[Fe_4S_4]^{2+}$ clusters.[22,23,31,34] Interestingly, in comparison with the corresponding spectrum of wild-type *Synechocystis* FTR (Figure 3A), the prominent shoulder observed in the high-energy line of the wild-type spectrum is almost invisible in the spectrum of the C87A FTR. To obtain a quantitative comparison with the wild-type FTR, the spectrum of the variant is analyzed also by assuming that it is a superposition of three quadrupole doublets with an intensity ratio of 1:1:2 corresponding to the three Fe sites, *a*, *b*, and *c*. (However, it should be noted that such a decomposition of the variant spectrum is not unique. The lack of resolution of the variant spectrum prohibits a unique decomposition of the spectrum.) The resulting parameters are listed in Table 1, and the corresponding theoretical simulations are shown in Figure 10. In comparison with the parameters of the wild-type FTR, the parameters obtained for sites *c* are

(34) Middleton, P.; Dickson, D. P. E.; Johnson, C. E.; Rush, J. D. *Eur. J. Biochem.* **1978**, *88*, 135−141.

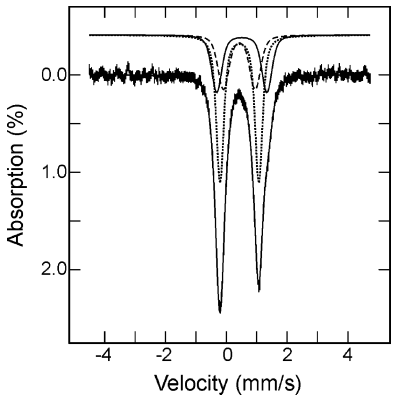

Figure 10. 4.2-K Mössbauer spectrum of *Synechocystis* C87A FTR recorded in a parallel field of 50 mT. The spectrum (hatched marks) is least-squares fitted to three quadrupole doublets with an intensity ratio of 1:1:2 representing three Fe sites *a*, *b*, and *c*. The resulting doublets are shown above the experimental spectrum as a solid line (site *a*), a dashed line (site *b*), and a dotted line (site *c*). The sum of the three doublets is shown as a solid line overlaid with the data. The parameters are listed in Table 1.

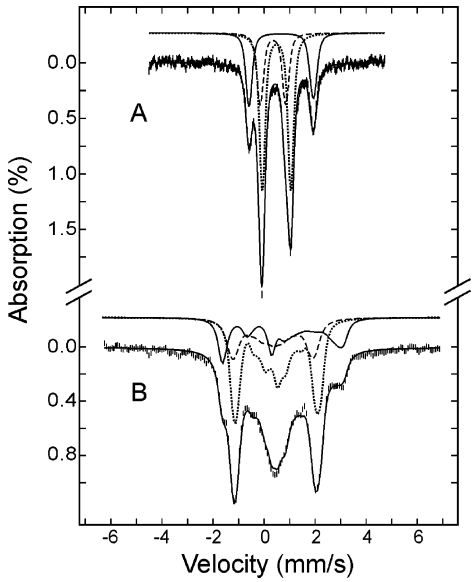

Figure 11. Mössbauer spectra of dithionite-reduced *Synechocystis* C57S FTR. The spectra (hatched marks) were recorded at 4.2 K in a parallel field of 50 mT (A) and 8 T (B). These spectra can be decomposed into three components with an intensity ratio of 1:1:2 representing a valence-localized $Fe^{2+}Fe^{3+}$ pair (sites *a* and *b*) and a valence-delocalized $Fe^{2+}Fe^{3+}$ pair (site *c*). A diamagnetic $S = 0$ ground state is assumed in this analysis. The theoretical simulations of the individual components are shown above the experimental spectra as solid lines (site *a*), dashed lines (site *b*), and dotted lines (site *c*). The sums of the three components are shown as solid lines overlaid with the experimental spectra. The parameters are listed in Table 1.

similar, while a decrease in the δ value of site *a* and an increase in the δ value of site *b* are observed. The difference between the δ values of sites *a* and *b* has reduced from 0.15 mm/s in the as-purified wild-type FTR to 0.08 mm/s in the C87A variant. Thus, on the basis of such an analysis, it is concluded that the C87A substitution has the effect of equalizing the charge distribution between sites *a* and *b*, resulting in a reduction of the ferrous character of the unique Fe site *a* making it more ferric like. This conclusion is consistent with the proposal that interaction between the cluster and the active-site disulfide (via Cys87) promotes the observed charge buildup at the unique Fe site in the resting enzyme.

C57S FTR can be reduced by dithionite, and the reduced protein shows optical spectra characteristic of a $[Fe_4S_4]^{2+}$ cluster.[13] Thus, the reduced C57S FTR provides an ideal system for studying the interaction between the $[Fe_4S_4]^{2+}$ cluster and the Cys87 residue free of restrictions caused by the disulfide bonding. The resonance Raman spectrum of reduced C57S shown in Figure 4C confirms the presence of a $[Fe_4S_4]^{2+}$ cluster. Moreover, the marked changes in the frequencies and relative intensities of Raman bands, as compared to the $[Fe_4S_4]^{2+}$ centers in oxidized FTR which has the disulfide intact (see Figure 4A) and C87A FTR which lacks both the disulfide and the cluster-interacting Cys87 (see Figure 4B), suggest that significant changes in cluster ligation and core structure are associated with having Cys87 as a free thiol in close proximity to the cluster. For example, the symmetric (breathing) mode of the Fe_4S_4 core is no longer the most intense resonance Raman band in reduced C57S FTR and is shifted to 335 cm^{-1}, as compared to 337 cm^{-1} in oxidized wild-type and C87A FTR, while the asymmetric Fe−S(Cys) stretching mode becomes the most intense band and is shifted to 356 cm^{-1}, as compared to 360 cm^{-1} in wild-type and C87A FTR, see Figure 4. In addition, pronounced frequency and intensity changes are apparent in the weak low-frequency asymmetric stretching modes of the Fe_4S_4 core in the 260−320 cm^{-1} region for the $[Fe_4S_4]^{2+}$ center in reduced C57S FTR.

Mössbauer studies of reduced C57S FTR revealed that the presence of Cys87 as a free thiol in close proximity to the $[Fe_4S_4]^{2+}$ center has a dramatic effect on the electronic properties of the cluster. Figure 11 shows the 4.2-K Mössbauer spectra of a dithionite-reduced C57S FTR sample recorded in a magnetic field of 50 mT (A) and 8 T (B) applied parallel to the γ-radiation. In addition to an intense central quadrupole doublet, which is similar to those of $[Fe_4S_4]^{2+}$ clusters, the weak-field spectrum (Figure 11A) shows a resolved outer quadrupole doublet that accounts for approximately 25% of the total Fe absorption. This outer doublet exhibits parameters ($\Delta E_Q = 2.52$ mm/s and $\delta = 0.67$ mm/s) that are indicative of a tetrahedral sulfur-coordinated high-spin ($S = 2$) ferrous center. The 8-T spectrum (Figure 11B) shows that both doublets originate from a diamagnetic $S = 0$ ground state, indicating unambiguously that the high-spin ferrous ion is an integral part of a diamagnetic Fe cluster. The percent absorption of this ferrous site further suggests that it represents one single Fe site of a $[Fe_4S_4]^{2+}$ cluster. Taken together, the data establish that the reduced C57S FTR contains a novel $[Fe_4S_4]^{2+}$ cluster with a valence-localized high-spin ferrous site. In line with assumptions used for analyzing the spectra of other $S = 0$ $[Fe_4S_4]^{2+}$ clusters in FTR, the spectra of reduced C57S FTR are also least-squares fitted with three quadrupole doublets of an intensity ratio of 1:1:2 corresponding to sites *a*, *b*, and *c*. The high-spin ferrous site is assigned to site *a*. The results are listed in Table 1. By comparing these parameters obtained for reduced C57S FTR with those of the as-purified wild-type FTR and C87A FTR, the effect of Cys87 on the charge distribution of the $[Fe_4S_4]^{2+}$ cluster in FTR can be clearly seen. The δ value of the unique Fe site *a* is observed to increase progressively from a minimum value of 0.51 mm/s in C87A FTR, in which Cys87 has been substituted by alanine, to a medium value of 0.54 mm/s in the as-purified FTR, in which Cys87 forms a disulfide with Cys57, and to a maximum value of 0.67 mm/s in reduced C57S FTR, in which Cys87 is free of disulfide bonding. Concomitantly, a gradual

decrease in the δ value of site *b* is observed (from 0.43 mm/s in C87A FTR, to 0.39 mm/s in as-purified FTR, to 0.35 mm/s in reduced C57S FTR). These data establish clearly that an interaction between the Cys87 residue and the $[Fe_4S_4]^{2+}$ cluster is indeed present in FTR and that the effect of this interaction is to polarize the charge distribution between the two Fe ions (sites *a* and *b*) of one of the two $Fe^{2+}Fe^{3+}$ mixed-valence pairs. In reduced C57S FTR, the residue Cys87 is free of disulfide bonding and thus the interaction is observed to generate a maximum effect, resulting in a novel $[Fe_4S_4]^{2+}$ cluster with a valence-localized $Fe^{2+}Fe^{3+}$ pair. In the as-purified enzyme, this interaction is weakened by bonding of Cys87 to Cys57, resulting in only a partial localization of the valence electron and ending with a charge buildup at the unique Fe site *a*. In C87A FTR, replacing Cys87 with a nonpolar alanine further diminishes the strength of the interaction between residue 87 and the cluster, resulting in an additional reduction of the charge difference between sites *a* and *b*. Interestingly, the valence-delocalized $Fe^{2+}Fe^{3+}$ pair (site *c*) in reduced C57S FTR also shows a significant increase in the δ value (0.49 mm/s). Thus, the overall δ value of the cluster in reduced C57S FTR (0.50 mm/s) is considerably higher and outside of the range of δ values (0.42−0.45 mm/s)[22] generally observed for a regular $[Fe_4S_4]^{2+}$ cluster. This observation indicates that the reduced C57S FTR contains a $[Fe_4S_4]^{2+}$ cluster that is more electronegative than regular $[Fe_4S_4]^{2+}$ clusters and suggests a possible additional function for residue Cys87 of promoting an overall charge buildup at the $[Fe_4S_4]^{2+}$ cluster.

Methyl Viologen-Reduced FTR. In the preceding section, dithionite-reduced C57S FTR has been shown to contain an unprecedented electron-rich $[Fe_4S_4]^{2+}$ cluster composed of a valence-localized and a valence-delocalized $Fe^{2+}Fe^{3+}$ mixed-valence pair. Because our spectroscopic data have also established that the as-purified C57S FTR represents a stable analogue of a one-electron-reduced FTR intermediate (see above), the dithionite-reduced C57S FTR must represent an analogue of two-electron-reduced FTR. In wild-type FTR, the active-site disulfide can be reduced by methyl viologen, but not by dithionite.[35] Moreover, reduced methyl viologen can function as the electron donor for catalytic turnover of FTR,[35] and the methyl viologen-reduced enzyme exhibits an optical spectrum indicative of a $[Fe_4S_4]^{2+}$ cluster and can form heterodisulfide complexes with Trx substrates. Thus, the methyl viologen-reduced FTR is likely to represent a catalytically competent two-electron-reduced form of FTR. To investigate whether the novel state of the $[Fe_4S_4]^{2+}$ cluster detected in reduced C57S FTR has any functional relevance, resonance Raman and Mössbauer spectroscopies were used to characterize methyl viologen-reduced FTR. The resonance Raman spectrum of *Synechocystis* FTR reduced with a 10-fold excess of reduced methyl viologen was identical to that shown in Figure 4C for dithionite-reduced C57S FTR, except for additional bands originating from excess reduced methyl violgen (data not shown). Figure 12A shows the Mössbauer spectrum (hatched marks) of spinach FTR reduced with a 3-fold excess of reduced methyl viologen recorded at 4.2 K in a 50-mT applied field. Detailed analysis of the spectrum shows that the sample contains approximately 14% as-purified FTR (i.e., enzyme that has not been reduced by methyl viologen). Removal of the contribution of the as-purified FTR (solid line in Figure 12A) from the raw data results in a spectrum representing the methyl viologen-reduced enzyme (Figure 12B). This spectrum is very similar to that observed for the reduced C57S FTR (Figure 11A). Most importantly, a resolved outer quadrupole doublet, typical of tetrahedral sulfur-coordinate high-spin ferrous ions and accounting for ∼25% of the Fe absorption, is clearly observable. This spectrum can also be least-squares fitted with three quadrupole doublets with an intensity ratio of 1:1:2. The resulting parameters are listed in Table 1. Within experimental uncertainties, these parameters are identical to those obtained for the reduced C57S FTR, establishing firmly that the two-electron-reduced FTR also contains a novel electron-rich $[Fe_4S_4]^{2+}$ cluster composed of valence-localized and valence-delocalized $Fe^{2+}Fe^{3+}$ pairs. The biological implications of this unique and unexpected type of $[Fe_4S_4]^{2+}$ cluster in two-electron-reduced FTR are discussed below.

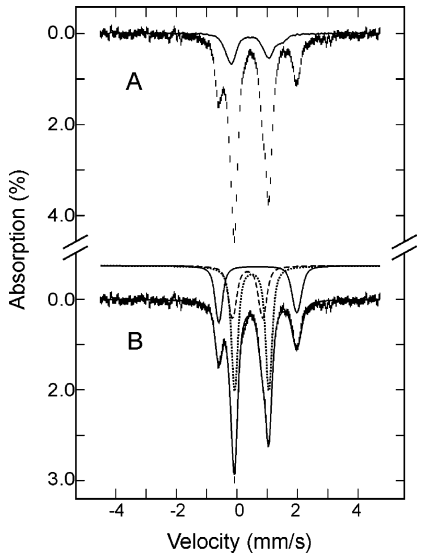

Figure 12. Mössbauer spectra of methyl viologen-reduced spinach FTR. Shown in (A) is the experimental spectrum (hatched marks) of a methyl viologen-reduced spinach FTR sample recorded at 4.2 K in a parallel field of 50 mT. Approximately 14% of the protein molecules in this sample remain in the as-purified state. The solid line in (A) is the spectrum of the as-purified FTR (Figure 1 of ref 11) normalized to 14% of the total Fe absorption of the reduced sample. Removal of the contributions of the as-purified proteins from the raw data yields the spectrum shown in (B) (hatched marks). This spectrum can be decomposed into three quadrupole doublets with an intensity ratio of 1:1:2 representing three distinct Fe sites *a*, *b*, and *c*. These doublets are shown above the experimental spectrum as a solid line (site *a*), a dashed line (site *b*), and a dotted line (site *c*). The sum of the three doublets is shown as a solid line overlaid with the experimental spectrum.

Redox Properties of NEM-FTR, C57S FTR, and Wild-Type FTR/Trx *m* Heterodisulfide Complex. Oxidized NEM-FTR can be reduced by dithionite or reduced benzyl viologen, and reduced NEM-FTR is EPR silent. Hence, dye-mediated EPR redox titrations provide a means of assessing redox potential and the number of electrons and protons involved in reducing NEM-FTR. Figure 13A shows redox titrations of *Synechocystis* NEM-FTR performed at pH 7.0 and pH 8.0 monitored by the intensity of the $g = 2.11$ EPR signal. The reduction−oxidation process at these pH values was found to be fully reversible. The solid lines shown in Figure 13A are least-squares fits to the data using a one-electron Nernst equation with midpoint

(35) Schürmann, P.; Stritt-Etter, A.-L.; Li, J. S. *Photosynth. Res.* **1995**, *46*, 309−312.

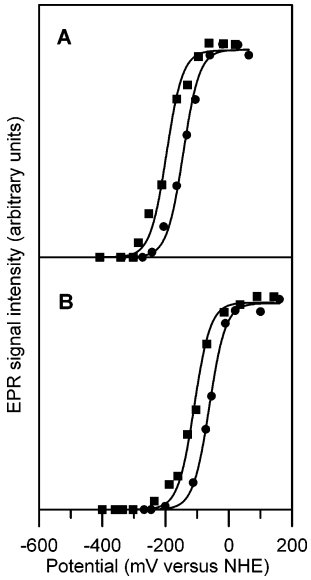

Figure 13. EPR-monitored redox titrations of *Synechocystis* NEM-FTR (A) and wild-type *Synechocystis* FTR/C40S Trx *m* heterodisulfide complex (B). Data points correspond to the intensity of the $S = {}^1/_2$ EPR from the $[Fe_4S_4]^{3+}$ center at pH 7.0 (●) and pH 8.0 (■). The initial concentration of enzyme used in each titration was 100 μM, and all data points have been normalized for dilution effects upon reductive titration with sodium dithionite. The solid lines are the best fits to one-electron Nernst equations with $E_m = -145 \pm 10$ mV (pH 7.0) and -200 ± 10 mV (pH 8.0) for NEM-FTR and $E_m = -60 \pm 10$ mV (pH 7.0) and -110 ± 10 mV (pH 8.0) for the FTR/C40S Trx *m* heterodisulfide complex.

reduction potentials of $E_m = -145 \pm 10$ mV and -200 ± 10 mV at pH 7.0 and pH 8.0, respectively.

This observed negative shift of the redox potential by approximately 60 mV/pH unit with increasing pH indicates that the one-electron reduction of NEM-FTR is coupled with the uptake of one proton. The protonation site is likely to be Cys87, because one-electron reduction of the $[Fe_4S_4]^{3+}$ cluster in NEM-FTR is proposed to result in cleavage of the Fe−S(Cys87) bond, see Figure 2. EPR redox titrations of *Synechocystis* C57S FTR showed the same redox properties as *Synechocystis* NEM-FTR, that is, one-electron redox process with $E_m = -145 \pm 10$ mV at pH 7.0 and -200 ± 10 mV at pH 8.0 (data not shown). An earlier EPR redox titration study of the spinach NEM-FTR reported a more negative redox potential of -210 ± 10 mV at pH 7.[8]

Analogous dye-mediated EPR-monitored redox titrations were also performed with the wild-type *Synechocystis* FTR/C40S Trx *m* heterodisulfide complex at pH 7.0 and 8.0, see Figure 13B. At both pH values, the titrations were fully reversible and the data were fit using a one-electron Nernst equation with midpoint reduction potentials of $E_m = -60 \pm 10$ mV (pH 7.0) and -110 ± 10 mV (pH 8.0). While the potentials are ~90 mV higher than for *Synechocystis* NEM-FTR, the pH-dependence again indicates that one-electron reduction is coupled with the uptake of one proton. The mechanistic scheme shown in Figure 2 proposes that one-electron reduction of the $[Fe_4S_4]^{3+}$ cluster-containing heterodisulfide intermediate results in cleavage of the Fe−S(Cys87) bond and concomitant reformation of the FTR disulfide coupled with cleavage of the heterodisulfide. Hence, the status of the heterodisulfide during a parallel dye-mediated redox titration at pH 7.3 was assessed by anaerobic chromatographic separation of FTR, C40S Trx *m*, and the FTR/C40S Trx *m* heterodisulfide complex for samples poised at selected

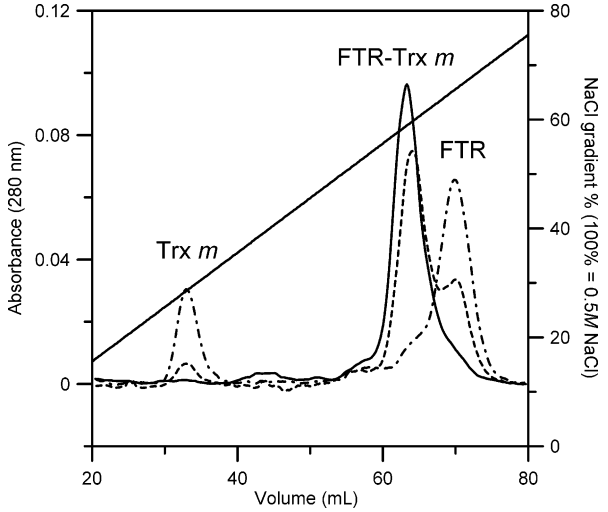

Figure 14. Chromatographic analysis of the status of the heterodisulfide in *Synechocystis* FTR/C40S Trx *m* heterodisulfide complex poised at selected potentials (vs NHE) in an EPR redox titration: solid line, +100 mV; dashed line, −85 mV; dot−dash line, −400 mV versus NHE. FTR/Trx *m* heterodisulfide complex at pH 7.3 was incubated in redox dyes and poised at various potentials according to procedure for EPR redox titrations as described in Materials and Methods. At specified potentials, an aliquot of sample was applied to a 5-mL High-Performance Q-Sepharose column and eluted with a gradient of 0.0−0.5 M NaCl in 20 mM triethanolamine-Cl buffer, pH 7.3.

potentials using a high-performance Q-Sepharose column. Samples were loaded onto the column at low salt, and protein fractions were eluted with a 0.0−0.5 M NaCl gradient. Elution profiles for samples poised at +100 mV, −85 mV (estimated midpoint potential of the complex at pH 7.3), and −400 mV are shown in Figure 14, and protein bands were identified by parallel chromatographic studies with oxidized forms of FTR, C40S Trx *m*, and the FTR/C40S Trx *m* heterodisulfide complex. The data unambiguously demonstrate that one-electron reduction of the complex with a midpoint potential of -60 ± 10 mV (pH 7.0) and -110 ± 10 mV (pH 8.0) results in the reversible cleavage of the heterodisulfide resulting in the ability to chromatographically separate FTR and Trx *m*. Hence, the protonation site is likely to be the thiolate that is generated on C40S Trx *m* on cleavage of the heterodisulfide.

Discussion

The primary objective of the spectroscopic studies of FTR reported herein was to evaluate the underlying assumptions of the mechanistic hypothesis shown in Figure 2 for $[Fe_4S_4]$-cluster-mediated disulfide reduction in two sequential one-electron steps. This scheme proposes distinct, noninterchangeable roles for cysteines of the active-site disulfide, site-specific cluster chemistry in the oxidized and one-electron-reduced intermediate, and the existence of a stable one-electron-reduced FTR/Trx heterodisulfide intermediate that undergoes further one-electron reduction leading to the reformation of the active-site disulfide and release of reduced Trx. These proposals have been comprehensively assessed via EPR, VTMCD, resonance Raman, Mössbauer, and redox studies of wild-type and NEM-modified forms of FTR, site-specific variants of each of the active-site cysteines, and of a heterodisulfide complex involving FTR and the C40S variant of Trx *m*.

The properties of the C57S and C87A FTR variants as compared to those of wild-type and NEM-modified FTR clearly

demonstrate distinct roles for the cysteine residues of the active-site disulfide. Both the C57S and the C87A variants are inactive, indicating that both cysteines of the active-site disulfide are essential for catalytic activity.[13] However, the C87A and C57S variants have entirely different spectroscopic and redox properties. C87A FTR contains a redox-inactive $[Fe_4S_4]^{2+}$ cluster, whereas C57S FTR contains a redox-active $[Fe_4S_4]^{3+/2+}$ center with spectroscopic and redox properties almost indistinguishable from those of the $[Fe_4S_4]^{3+/2+}$ center in NEM-FTR. Moreover, in accord with our preliminary Mössbauer analysis,[11] the unique spectroscopic properties of the $[Fe_4S_4]^{3+}$ cluster in NEM-FTR can only be rationalized in terms of selective oxidation at a unique Fe site resulting from coordination of Cys87 to yield a five-coordinate Fe site. In accord with the mechanism depicted in Figure 2, the mutagenesis results, therefore, identify Cys87 as the cluster-interacting thiol and demonstrate that Cys57 cannot assume this role in the C87A variant. In addition, the ability of C87A, but not C57S FTR, to form a heterodisulfide complex with active-site variants of Trxs,[13] identifies Cys57 as the interchange thiol responsible for attacking the Trx disulfide.

The spectroscopic properties of the C87A variant also support the proposal for a weak interaction between the active-site disulfide and the unique Fe site of the $[Fe_4S_4]^{2+}$ cluster in the oxidized resting state of FTR. Mössbauer studies of spinach[11] and *Synechocystis* FTR in the oxidized resting state suggest that the asymmetrically disposed disulfide is responsible for promoting charge buildup on the unique Fe site, resulting in a $[Fe_4S_4]^{2+}$ cluster comprising one fully valence-delocalized $Fe^{2+}Fe^{3+}$ pair and one partially valence-delocalized $Fe^{2+}Fe^{3+}$ pair. This conclusion is substantiated by the observation that the loss of the disulfide in the C87A variant results in a $[Fe_4S_4]^{2+}$ cluster that more closely approximates a conventional Fd-type $[Fe_4S_4]^{2+}$ cluster with two valence-delocalized $Fe^{2+}Fe^{3+}$ pairs. Any residual charge asymmetry in one of the valence-delocalized pairs in the C87A variant, see Table 1, is likely to be a consequence of the anomalous coordination geometry at the unique Fe site (see Figure 1). Hence, the interaction between the cluster and the active-site disulfide (via Cys87) promotes the observed charge buildup at the unique Fe site in the resting enzyme and primes the active-site for one-electron reduction leading to cleavage of the disulfide and attachment of Cys87 at the unique Fe site.[11]

Characterization of the oxidized form of the wild-type FTR/C40S Trx *m* heterodisulfide complex reveals a form of FTR that is spectroscopically indistinguishable from oxidized NEM-FTR. This observation is entirely consistent with the proposal for a one-electron-reduced heterodisulfide intermediate containing a $[Fe_4S_4]^{3+}$ cluster in which Cys87 is ligated to yield a five-coordinate Fe site and Cys57 is part of the heterodisulfide, see Figure 2. Moreover, the viability of this species as a stable analogue of the one-electron-reduced catalytic intermediate is confirmed by redox studies, which reveal that one-electron reduction of the FTR/C40S Trx *m* heterodisulfide complex ($E_m = -60 \pm 10$ mV at pH 7.0 and -110 ± 10 mV at pH 8.0) results in cleavage of the heterodisulfide coupled with protonation of free thiolate on C40S Trx *m*. Parallel redox studies of NEM-FTR show a similar one-electron reduction, albeit at lower potentials ($E_m = -145 \pm 10$ mV at pH 7.0 and -200 ± 10 mV at pH 8.0) due to increased solvent exposure at the active site in the absence of Trx, and in this case the pH dependence is attributed to release and protonation of Cys87 on reduction. Taken together, these redox results suggest that cleavage of the heterodisulfide occurs via reductive release of Cys87 and subsequent nucleophilic attack of the heterodisulfide by Cys87, resulting in cleavage of the heterodisulfide and reformation of the active-site disulfide, as shown in Figure 2.

Interestingly, a much lower redox potential ($E_m = -280$ mV at pH 7.0) was determined for cleavage of the heterodisulfide in the *Synechocystis* wild-type FTR/C40S Trx *m* heterodisulfide complex using dithiothreitol (DTT), a two-electron reductant that is particularly effective in cleaving disulfides.[13] These redox titrations involved poising samples of the heterodisulfide complex at specific potentials using mixtures of oxidized and reduced DTT and assessing cleavage of the heterodisulfide using native gel electrophoresis to separate FTR, Trx, and the FTR/Trx heterodisulfide complex. The difference in potentials presumably reflects the efficacy of cleaving the heterodisulfide with a one-electron donor via reduction of the $[Fe_4S_4]^{3+}$ cluster as compared to direct two-electron cleavage of the heterodisulfide using dithiol/disulfide chemistry. This rationalization of the redox properties has since been verified by subsequent experiments in which the cleavage reaction of the heterodisulfide using a 2500-excess of reduced DTT showed a long lag phase of about 50 min before a separation of the proteins, accompanied by a change in absorption properties of the $[Fe_4S_4]^{3+}$ cluster, is observed (unpublished observations). The high potential for the one-electron reduction and cleavage of the heterodisulfide in the oxidized FTR/C40S Trx *m* complex ($E_m = -110 \pm 10$ mV at pH 8.0, the physiological pH of light-adapted chloroplasts) suggests that the second reducing equivalent used by FTR need not be derived from reduced Fd and may not require a specific electron donor. This is in accord with the observation that ferredoxin is not obligatory for cleaving the heterodisulfide and that other potential physiological electron donors such as a NADPH and ferredoxin:$NADP^+$ reductase can act as effective reductants in vitro.[13]

The most interesting and unexpected result to emerge from these spectroscopic studies of FTR concerns the properties of the $[Fe_4S_4]^{2+}$ cluster in the two-electron-reduced form of FTR. Reduced methyl viologen is known to reduce the active-site disulfide and is a catalytically competent reductant for FTR.[35] Both Mössbauer and resonance Raman studies confirm the presence of a $S = 0$ $[Fe_4S_4]^{2+}$ cluster in methyl viologen-reduced FTR, with Mössbauer revealing an unprecedented type of electron-rich $[Fe_4S_4]^{2+}$ cluster composed of both valence-localized and valence-delocalized $Fe^{2+}Fe^{3+}$ pairs and resonance Raman indicating significant structural changes in the ligation and core structure of the cluster as compared to the $[Fe_4S_4]^{2+}$ clusters in oxidized forms of FTR. A species with analogous Mössbauer and resonance Raman properties is also observed in the dithionite-reduced C57S FTR, which can be regarded as a two-electron-reduced analogue that is lacking Cys57. Moreover, the pH-dependence of the redox potentials of NEM-FTR and C57S FTR strongly suggests that Cys87 dissociates and becomes protonated on one-electron reduction. Hence, the unique properties of the $[Fe_4S_4]^{2+}$ cluster in two-electron-reduced forms of FTR are likely to result, at least in part, from the presence of a free thiol (Cys87) in close proximity to the cluster. Our interpretation of the anomalous properties of the $[Fe_4S_4]^{2+}$ cluster in two-electron-reduced FTR is that they

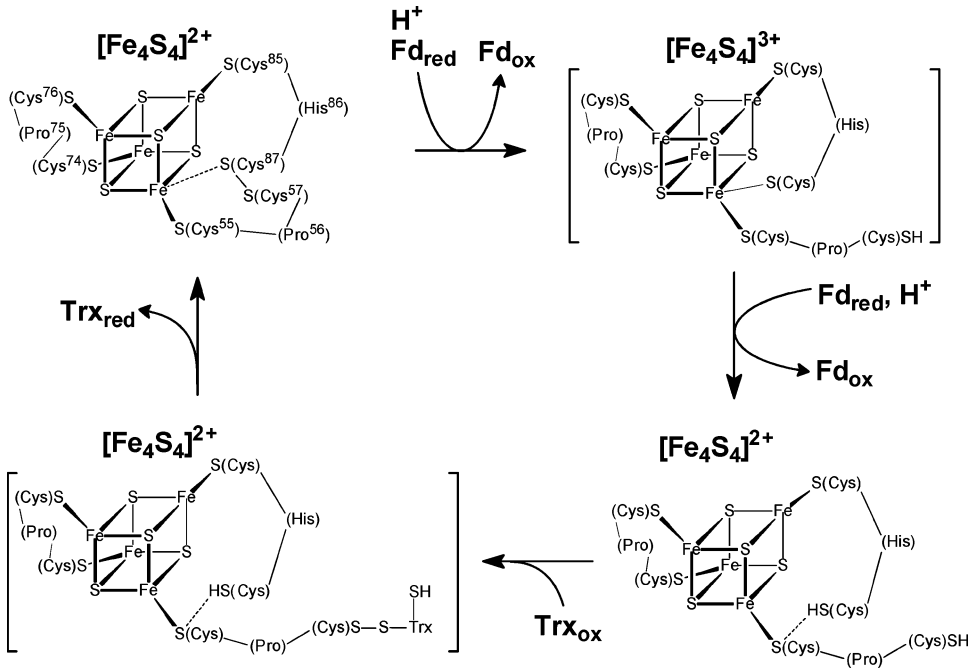

Figure 15. Alternative proposal for the catalytic mechanism of FTR. Residue numbering is for *Synechocystis* FTR. Square brackets are used to indicate transient intermediates.

originate in large part from a strong H-bonding interaction between the thiol form of Cys87 and the coordinated S atom of Cys55. A substantial increase in H-bonding interactions involving the coordinated cysteinyl-S would be expected to promote charge build up at the unique Fe site, thereby creating a valence-localized $Fe^{2+}Fe^{3+}$ pair and an electron-rich $[Fe_4S_4]^{2+}$ cluster.

The discovery of site-specific cluster chemistry in the two-electron-reduced form of FTR raises an alternative possibility for the catalytic mechanism in which FTR is reduced by two electrons prior to interaction with Trx, see Figure 15. This mechanism invokes a transient one-electron-reduced intermediate with properties analogous to oxidized NEM-FTR and C57S FTR, as observed in freeze-quench studies under turnover conditions and during reduction with stoichiometric reduced methyl viologen,[10] but this intermediate is reduced to yield the two-electron-reduced species prior to interaction with Trx. The strong H-bonding interaction anchors the cluster-interacting thiol Cys87, in the two-electron-reduced form thereby freeing the interchange thiol Cys57 for nucleophilic attack of Trx. Hence, the substrate disulfide is cleaved via conventional dithiol/disulfide chemistry, with the cluster playing a role in facilitating disulfide reduction in two sequential one-electron steps and in anchoring the cluster-interacting thiol to facilitate the initial nucleophilic attack by the interchange thiol. In many respects, this mechanism is very similar to that found in the more extensively studied nucleotide-dependent disulfide reductases,[4−6] with the $[Fe_4S_4]^{2+}$ cluster performing the role of the flavin in anchoring one of the active-site thiols to free the other for attacking the substrate disulfide. The major difference resides in the use of a $[Fe_4S_4]^{2+}$ cluster to facilitate active-site disulfide reduction using a one-electron donor.

The primary rationale for invoking formation of the heterodisulfide intermediate at the one-electron-reduced level in the mechanistic scheme proposed in Figure 2 was that attachment of the cluster interacting thiol, Cys87, frees the interchange thiol for nucleophilic attack and cleavage of the Trx disulfide. Clearly, a strong H-bonding interaction involving the cluster interacting thiol can perform the same function in the two-electron-reduced form. The alternative mechanism is also clearly viable because reductants such as reduced methyl viologen that rapidly cleave the active-site disulfide have been shown to be catalytically competent electron donors.[35] Moreover, this mechanism obviates the need for Fd/FTR/Trx triple complex as part of the catalytic mechanism and enables the light-mediated generation of a pool of two-electron-reduced FTR that is always available for Trx reduction. Nevertheless, as demonstrated in this work, there is now good evidence for a catalytically competent one-electron-reduced heterodisulfide intermediate, and it is not possible to discriminate between the mechanistic proposals shown in Figures 2 and 15 on the basis of the currently available evidence. Future studies are planned to address this question and characterize the role of the conserved His86 in the active-site acid−base chemistry.

Acknowledgment. his work was supported by grants from the National Institutes of Health (GM62542 to M.K.J., GM47295 to B.H.H.) and from the Swiss National Science Foundation (grant nos. 31-56761.99 and 3100-067934 to P.S.).